Laser and Particle Beams (2011), *29*, 113–119.

doi:10.1017/S0263034611000103

Revealing of hydrodynamic and electrostatic factors in the center-of-mass velocity of an expanding plasma generated by pulsed laser ablation

J. KRÁSA,[1] A. LORUSSO,[2] V. NASSISI,[2] L. VELARDI,[2] AND A. VELYHAN[1]

[1]Institute of Physics, ASCR, Prague, Czech Republic
[2]Department of Physics of Lecce, Laboratorio di Elettronica Applicata e Strumentazione, INFN of Lecce, Lecce, Italy

(Received 14 July 2010; Accepted 15 January 2011)

Abstract

Time-of-flight spectra of C, Fe, and Si ions produced with the use of a KrF excimer laser have been analyzed. Ion currents were collected by Faraday cups and their responses were analyzed using a detector signal function. This function was derived from shifted Maxwell-Boltzmann velocity distribution, in order to uncover the contribution of partial currents of all the ionized species constituting the expanding plasma plume. The deconvolution method allowed to estimate parameters of the plasma, such as the ion temperature and the center-of-mass velocities of expanding ionized species. Furthermore, the linear charge-state dependence of the center-of-mass velocity has revealed the contribution of hydrodynamic and electrostatic forces to the expansion velocity of the plasma. The nearly isotropic distribution of the center-of-mass velocity indicates that the shape of the plasma plume is determined mainly by the angular distribution of the ionization degree of ions.

Keywords: Angular distribution of ions; Faraday cup signal function; Partial ion currents

1. INTRODUCTION

The shape of time-resolved ion collector signals induced by ions from laser-produced plasma reflects changes in the velocity distribution of ions during their expansion into the vacuum. The initial phase of plasma expansion is formed by the evolution of the hierarchy of processes occurring during and after the interaction of the laser pulse with the matter — by a pressure gradient, various electrical driving forces, and gradients of potentials, as e.g., target normal sheath acceleration, skin-layer ponderomotive acceleration, double-layer effect in the expanding plasma (Tajima & Dawson, 1979; Gitomer *et al.*, 1986; Haseroth & Hora, 1996; Badziak *et al.*, 1999; Wilks *et al.*, 2001; Torrisi *et al.*, 2002; Hora 2007; Láska *et al.*, 2009; Liu *et al.*, 2009). Currently, the investigation of the early formation of plasma jets has become an interesting object for theoretical and experimental investigation for ion acceleration (Kasperczuk *et al.*, 2008, 2009; Andreev *et al.*, 2009; Bin *et al.*, 2009; Steinke *et al.*, 2010). For the analysis and interpretation of experimental data, a real complex of studies is needed. Nevertheless, a decisive criterion for the interpretation of the experimental data is the distance of the probe from the target surface. For example, if the optical emission spectroscopy is applied for measuring the temporal evolution of plasma parameters at a fixed distance of a few millimeters to centimeters, a theoretical model taking into account a hierarchy of processes as well as a non-Maxwell velocity distribution should be a base for the data interpretation (Capitelli *et al.*, 2004). If the probe is positioned outside the recombination zone ($L > L_{CR}$, where L_{CR} is the critical distance), the temperature is established, ion charge-states are frozen and ions freely drift into the vacuum. The determination of the critical distance is based on the analysis of ion currents, $j(t)$ (i.e., time-of-flight (TOF) spectra), and of the total charge, Q, carried by ions using expressions $t_{L1} = (L_1/L_2)\, t_{L2}$; $j_{L1} = (L_1/L_2)^3 j_{L2}$ and $Q_{L1} = (L_1/L_2)^2 Q_{L2}$, which allow to compare TOF spectra observed at different distances L_1 and L_2. Far from the target, i.e., for $L > L_{CR}$, both the ion current and the total charge decrease with increasing L as $j(t) \propto L^{-3}$ and $Q \propto L^{-2}$, respectively. This analysis was demonstrated experimentally for Cu plasma produced with the use of 308-nm excimer laser (Lorusso *et al.*, 2005). Since it

Address correspondence and reprint requests to: J. Krása, Institute of Physics, ASCR, Na Slovance 2, 18 221 Prague 8, Czech Republic. E-mail: krasa@fzu.cz

was experimentally proven that recombination and collisional excitation processes are not important in the last zone of expansion, one can suppose that the Maxwell-Boltzmann shifted distribution of ions well characterizes the motion of ions far from the target (Lorusso *et al.*, 2006).

The aim of our work is to analyze TOF spectra of ions, which is based on an ion collector signal function derived from a shifted Maxwell-Boltzman velocity distribution function. The signal function allows the uncovering of the partial ion currents from the ion collector signal and the distinguishing of the components of the center-of-mass (CM) velocity induced by hydrodynamic and electrostatic forces. Thermal ions were generated with the use of a KrF laser delivering the intensity of about 10^8 W/cm^2 onto a target.

2. SIGNAL FUNCTION OF ION COLLECTOR

The diagnostics of expanding laser-produced plasma is based on the analysis of TOF spectra. The expression for the detector's signal was originally deduced for expanding neutral species into the vacuum considering an ablated flux $d\vec{v}\times v_x dN$ of particles characterized by a Maxwell-Boltzmann velocity distribution function $f_{MB}(\vec{v})$ (Kelly & Dreyfus, 1988; Miotello & Kelly, 1999). This procedure was applied to derive a signal function equivalent to the current density of ions having a velocity distribution $f(\vec{v})$:

$$j_{IC}(t) \propto v_x f(\vec{v})\, d\vec{v} \propto \frac{L^2}{t^5} f\left(\frac{L}{t}\right), \tag{1}$$

where it is assumed that the ion collector is located at a distance $x = L$ from the target and the y, z directions are considered parallel to the target surface (Krása *et al.*, 2007, 2009). Furthermore, $v_x = L/t$, $|dv_x| = Ldt/t^2$, $dv_y = dy/t$, $dv_z = dz/t$ and the detector size is $dS = dzdy$. Thus, $d\vec{v} = (L/t^4)\, dSdt$. The influence of the center-of-mass (CM) motion of the plasma plume on the movement of ions can be expressed by a shifted velocity distribution $f(\vec{v} - \vec{u}_{CM})$, where $\vec{u}_{CM}$ is the CM velocity. Finally, the ion current is the sum of partial currents $j_{i,q}$ of all ionized species, i, with a charge-state, q. Then the total current density can be expressed as:

$$j_{IC}(L, t) = \sum j_{i,q}(L, t) = L^2 t^{-5} \sum j^0_{i,q} f_{i,q}\left(\frac{L}{t} - u_{i,q}\right), \tag{2}$$

where $j^0_{i,q}$ is the term for calibration of the peak amplitude of partial currents.

The presence of hydrodynamic and electrostatic forces in the expanding plasma can be established by analysis of values of all velocities $u_{i,q}$ obtained by fitting Eq. (2) to the TOF spectrum as both the forces contribute to u_{CM} by particular components (Torrisi *et al.*, 2002):

$$u_{CM} = u_{HD} + u_{EL}, \tag{3}$$

where u_{HD} is the velocity component corresponding to the effect to hydrodynamic forces, while u_{EL} is the velocity contribution deriving from the presence of the ambipolar electric field. Since the term u_{HD} is a part of the total CM velocity, u_{HD} is not related to the temperature of the ablated neutral gas (Kelly & Dreyfus, 1988; Miotello & Kelly, 1999).

The u_{CM} velocities as well as the kinetic energy of ionized species are quantities reflecting the acceleration of ions by fast electrons. For thermal ions generated by laser intensities lower than a threshold value of about 1×10^{14}W cm^{-2} (Gitomer *et al.*, 1986; Láska *et al.*, 2007*a*, 2007*b*) the charge-state dependence of u_{CM} was established experimentally (Krása *et al.*, 2007) as:

$$u_{CM}(q) = u_0 + u_q q. \tag{4}$$

This linear charge-state dependence of u_{CM} reflects the dominant effect of collisions on slowing down the acceleration of ions because the relative velocity $\Delta u \equiv u_2 - u_1$ of the species 1 and 2 in the collisional regime is:

$$\Delta u = (q_2 - q_1)\frac{eE}{m\omega}, \tag{5}$$

where E is the ambipolar electric field responsible for the ion acceleration and ω is the collision frequency between the species of the kinds 1 and 2, which decreases the contribution of the acceleration, as derived by Forslund (1980). Finally, comparing Eq. (3) and Eq. (4) the term u_0 may be interpreted as the term u_{HD}. Than the signal function (2) takes the form:

$$\begin{aligned} j_{IC}(L, t) = \sum j_{i,q}(L, t) = L^2 t^{-5} \sum j^0_{i,q} \exp \\ \times \left\{-\frac{m_i}{2kT}(L/t - u_{HD} - u_i q)^2\right\}, \end{aligned} \tag{6}$$

where m_i is the atomic mass of the i^{th} ion species, k is the Boltzmann constant, T is the equivalent ion temperature, and $u_i q$ represents u_{EL} in (3).

In contrast to the thermal ions, the fast ions exhibit different charge-state dependence because no "friction" forces balance the effect of the electric field as they do in the case of thermal ions (Krása *et al.*, 2009). The analysis of TOF spectra of fast ions generated by intensity $I > 1 \times 10^{14}$ W cm^{-2} shows that the $u_{CM}(q)$ dependence can be expressed as:

$$u_{CM}(q) = u_0 + u_q \sqrt{q}. \tag{7}$$

Both the dependencies (4) and (7) indicate, respectively, the limits for a strong or insignificant influence of ion-ion collisions and recombination on acceleration of ions by fast electrons.

3. EXPERIMENTAL SETUP

C, Fe, and Si plasmas were generated with the use of a KrF excimer laser (Lambda Physics, Compex) operated at

https://doi.org/10.1017/S0263034611000103 Published online by Cambridge University Press

248-nm wavelength. Laser pulses of 23 ns in duration were tilted by 70° with respect to the target normal. The focus spot area was about 1×10^{-3}cm^2 and the focused fluence ranged up to 120 J/cm^2. A set of Faraday cups (FC) was placed in front of the target at a distance ranging from 9 cm to 24 cm as shown in Figure 1. The operating circuit of FC was described by Doria *et al.* (2004).

The cups are 9 mm in diameter and 11.5 mm in distant from each other. Such configuration is able to diagnose the radial profile of the expanding plasma from −30° up to +30° with respect to the target normal direction for the 9-cm distance of the FC to the target. All the cups are inserted in the grounded flange, insulated among them and coaxially connected to a BNC (Bayonet Neill-Concelman) connector of 50Ω, which is able to derive the ion current signal to the oscilloscope.

4. RESULTS AND DISCUSSION

4.1. Ion Emission along Target Normal

Typical pulse-to-pulse fluctuations of time-resolved currents (TOF spectra) are shown in Figure 2a for ions emitted from a C plasma generated with a laser fluence of 12.5 J/cm^2. The TOF signals were observed in the direction of the target normal ($\phi = 0°$). Partial currents of C^{q+} ions uncovered by deconvolution of a TOF spectrum using Eq. (3) are shown as an example in Figure 2b. The best fit was obtained when besides the partial currents of C^{q+} $(1 \le q \le 4)$ ions also the contribution of a particular group of slow C^+ ions was included into the tail of the TOF spectrum. We note that the presence of this particular group of slow singly-charged ions is a general characteristic of all IC signals induced by impacting ions generated by sub-joule laser beams. Fitted values of u_{CM} (q) velocity are plotted in Fugure 3.

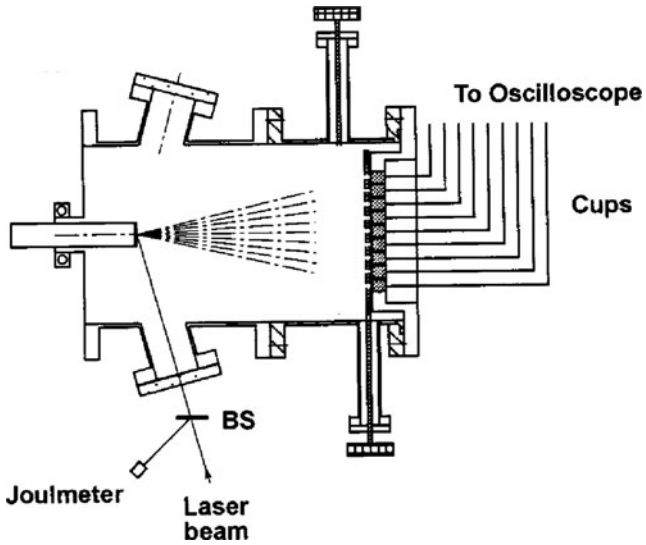

Fig. 1. Scheme of the experimental apparatus equipped with Faraday cups array placed in front to the target. A beam splitter (BS) is utilized in order to measure the laser energy by a joule meter.

The pulse-to-pulse fluctuations of the ion emission result in variations not only of the ion current and the total charge carried by them but also of the ion temperature and corresponding CM velocities, as Table 1 summarizes. The most affected characteristics of ions by pulse-to-pulse fluctuations are the ion temperature and CM velocity following the fluctuations of the width of TOF spectrum, which corresponds to the total charge carried by ions. The mean values of the fitted parameters in Eq. (6) are: $T = 2.6$ eV, $u_{HD} = 6.8 \times 10^3$ m/s, and $u_q = 8.1 \times 10^3$ m/s. The linear regression of the obtained values of u_{CM} clearly shows that the linear function (4) can be used as a suitable model in which the term u_0 can be interpreted as a part of u_{HD} corresponding to the hydrodynamic forces, while the term $u_q q$ reflects the electric forces, which are responsible of the acceleration of C^{q+} ions.

4.2. Energy Dependence of CM Velocity

The dependence of u_{CM} on the deposited laser energy was measured for Fe ions. Figure 4 shows an example of uncovered partial currents of Fe^{q+} $(1 \le q \le 5)$ ions generated with fluence of 122 J/cm^2. It is obvious that the dominant peak is constituted by Fe^{2+} ions. An entirely insignificant peak at TOF $\cong$ 7 μs is constituted by Fe^{5+} ions. Nevertheless, the corresponding value of u_{CM} (5) well matches the linear charge-state dependence plotted in Figure 4b. The dependence of obtained values of u_{HD} and u_q velocities on the laser fluence is shown in Figure 5. The values of u_{HD} are about six times lower than the u_q values, and u_{HD} exhibits weaker increase with the increasing laser fluence than u_q does.

The deconvolution of TOF current signals also allowed the determination of the ion temperature as a function of the laser fluence, as Figure 6 shows. Evidently, the temperature increases much more than u_q (see Fig. 5). Similar increase is exhibited by the peak current or by the total charge carried by ions.

4.3. Angular Distribution of Ion Emission

The angular distributions of ion peak current or the charge of ions is expressed by the following function:

$$S(\phi) = a\cos(\phi - \phi_0) - b\cos^n(\phi - \phi_0), \tag{8}$$

where $S(\phi)$ is the density of particles in the zenithal direction (ϕ) and a, b, and ϕ_0 are fit parameters (Thum-Jäger & Rohr, 1999; Láska *et al.*, 2008). The first term of Eq. (6) concerns the contribution of multiply charged particles with a rapid diminishing of a parameter during the ions' charge-state increasing: if $q \ge 2$, then the angular distribution $S(\phi)$ can be well described by the cos^n alone (Thum-Jäger & Rohr, 1999).

https://doi.org/10.1017/S0263034611000103 Published online by Cambridge University Press

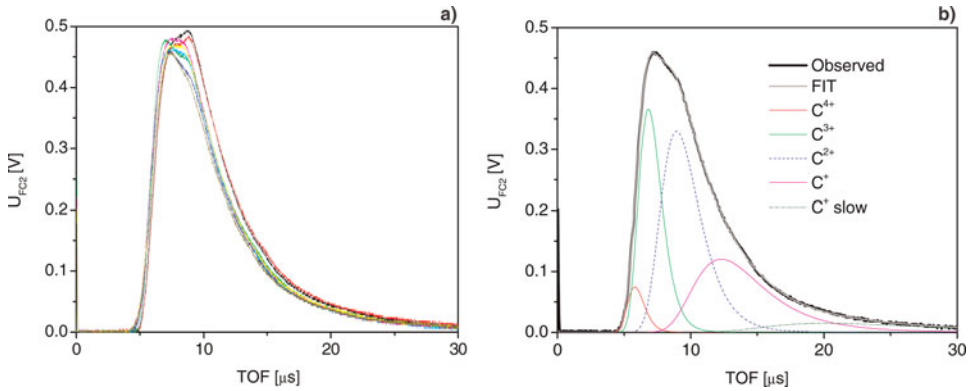

Fig. 2. (Color online) Pulse-to-pulse fluctuations of TOF spectra of C ions generated with 12.5 J/cm^2 fluence focused onto a graphite target (**a**). Deconvolution of TOF spectrum using the Faraday cup signal function (6); the uncovered peaks are ascribed to partial currents of C^{q+} $(1 \le q \le 4)$ ions (**b**). The distance of the Faraday cup from the target was 24 cm.

An example of angular distribution of the peak current (maximum value of the time-resolved current) of Si ions generated by 8-J/cm^2 laser fluence is shown in Figure 7. It is evident that the direction of the ions emission slightly turns toward the direction of the incoming laser beam as observed in other experiments (Thum-Jäger & Rohr, 1999; Láska *et al.*, 2008). We should note that the declination from the target normal direction is not a general phenomenon arising from the laser beam interaction with the expanding plasma. In our measurements, the angular distribution was observed only for the range of angles from 30° to −30° with respect to the target normal due to constraints given by the dimensions of the interaction chamber (Fig. 1).

The angular distribution of the ion current is formed by angular distributions of ion velocity and of charge curried by ions, as Figure 8 shows. Values of velocities u_{PEAK}, u_{HD}, and u_q as well as total charge Z_q of Si^{q+} $(1 \le q \le 4)$ ions were obtained by uncovering the partial ion currents from TOF spectra (Figs. 2 and 4). Figure 8a shows that the angular distribution of the charge of ions is similar in shape to the ion current distribution (Fig. 7) but the currents of Si^{3+} and Si^{4+} ions are not detectable at $\phi = 28°$, as Figure 9 demonstrates. Conversely, velocities u_{PEAK}, u_{HD}, and u_q exhibit a weak angular dependence, as Figure 8b shows. The value of the ratio of the lowest velocity to the highest one $u_{PEAK}(28°)/u_{PEAK}(343°) = 0.67$ is about four times higher than the value of the corresponding ratio of peak currents $j_{PEAK}(28°)/j_{PEAK}(343°) = 0.16$. Strong variations in angular distribution of ion currents are mainly caused by the narrow angular distribution of the charge curried by ions having the highest charge-states; the width of the stream of ions, in fact, decreases with increasing ion charge-state (Thum-Jäger & Rohr, 1999). Figure 9 demonstrates this effect for TOF spectra observed at $\phi = 343°$ and 28°. Evidently, two peaks of partial ion currents are absent in the TOF spectrum observed at $\phi = 28°$ for TOF ranging from about 2 μs to about 4 μs. A small difference between the summa of uncovered Si^{2+} and Si^{+} peaks for $\phi = 343°$ and the TOF spectrum observed at 28° elucidates small variations in both the angular distributions of u_{HD} and u_q velocities.

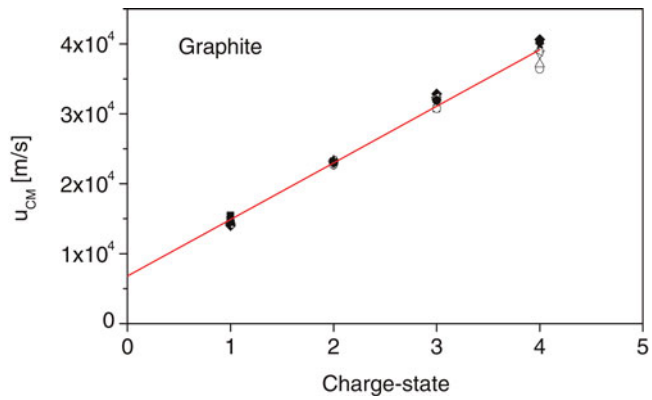

Fig. 3. (Color online) Charge-state dependence of fitted values of u_{CM} velocity of C^{q+} $(1 \le q \le 4)$ ions composing the hidden partial currents (see Fig. 1).

Another example of significant variations in the angular distribution of the partial currents emitted from a C plasma is shown in Figure 10. While along the target normal the partial currents of C^{+} to C^{4+} ions are emitted, the number of charge-states is reduced from 4 to 3 as well as the total number of C ions significantly decreases in the direction $\phi = 11°$. The small decrease of peak velocities of C^{q+} ions correlates with the small decrease of velocities of Si^{q+} ions, as Figure 8b confirms. Considering other observed angular distributions (Thum-Jäger & Rohr, 1999; Láska *et al.*, 2008) one can compile that the angular distribution

Table 1. *Standard deviations of parameters of ion-currents due to pulse-to-pulse fluctuations*

Parameters	Peak ion current	Total charge	Ion temperature	Velocity u_{HD}	Velocity u_q
Standard deviation	±2.6%	±4.6%	±12.8%	±16.4%	±7.8%

https://doi.org/10.1017/S0263034611000103 Published online by Cambridge University Press

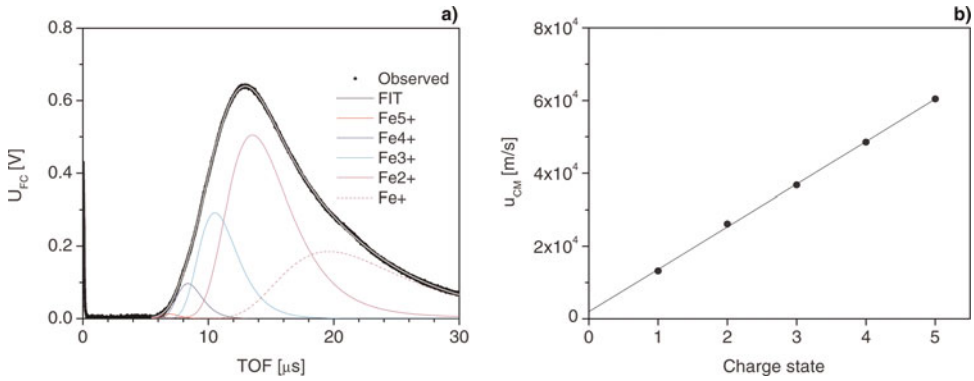

Fig. 4. (Color online) Partial currents of ion Fe^{q+} uncovered from TOF spectrum of ions produced with KrF laser beam delivering the fluence of 122 J/cm^2 onto Fe target; L = 44 cm (**a**). Charge-state dependence of u_{CM} for Fe^{q+} ($1 \le q \le 5$) ions (**b**).

of the number of ionized species $N_q(\phi)$ significantly affects the angular distribution of ion emission driven by laser pulses.

This phenomenon forms a characteristic behavior of expanding laser-produced ion beams. The jet-like structure of an ion current observed is shaped by the jet structure mainly of partial currents of ions with the highest charge-states. Since the CM velocity of all the ionized species constituting the plasma plume exhibit insignificant angular distribution, the shape of the plasma plume corresponds to the angular distribution of the charge states. The width of the expanding plasma is inversely proportional to the highest charge-state generated inside the plasma, as Figures 9 and 10 demonstrate and an empirical law for the atomic mass dependence of the exponent $n \approx A^{3/4}$ in Eq. (8) specifies (Thum-Jäger & Rohr, 1999).

As for the peak velocity u_{PEAK}, which belongs to the maximum of the total current $j(t)$, its value merely reflects the velocity of ions having the highest partial current $j_q(t)$ (Figs. 9 and 10). Thus, u_{PEAK} corresponds to the velocity $u_{CM} = u_q\, q$ of ion groups reaching the highest value of the current at the end of the recombination zone. It is useful to note that the peak velocity of the expanding plasma does not correlate with a mean velocity $<u>$ corresponding to the mean charge-state $<q>$ which was determined by the uncovering the partial ion currents to be $<q> = 2.3$. The value of $<u>$ is lower than u_{peak} about 0.75 times as can be estimated from Figure 9.

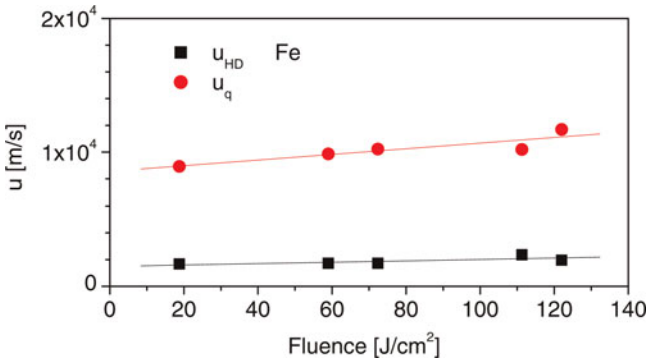

Fig. 5. (Color online) Dependence of u_{HD} and u_q of Fe^{q+} ions on laser fluence.

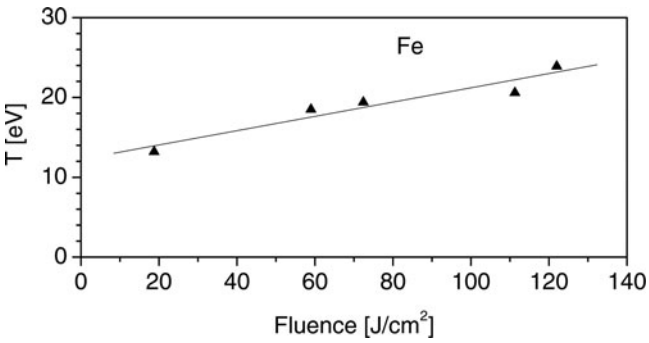

Fig. 6. Dependence of ion temperature of Fe^{q+} ions on laser fluence.

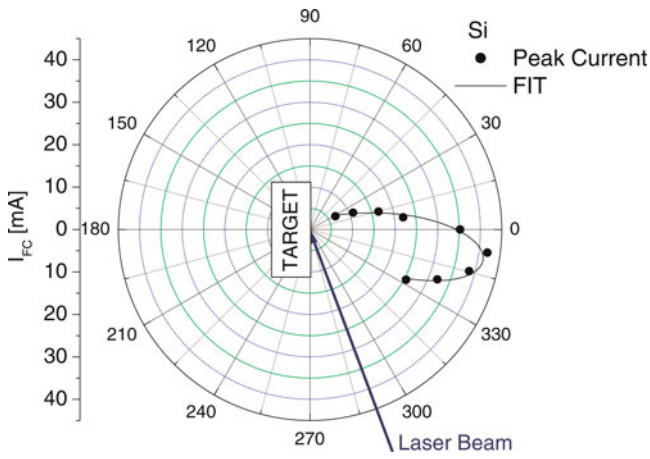

Fig. 7. (Color online) Angular distribution of peak current of Si ions generated with a laser fluence of 8 J/cm^2.

https://doi.org/10.1017/S0263034611000103 Published online by Cambridge University Press

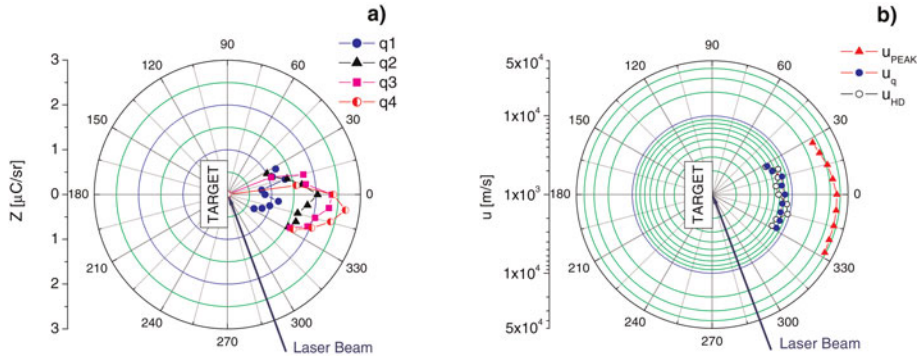

Fig. 8. (Color online) Angular distribution of (**a**) total charge Z curried by Si^{q+} ($1 \le q \le 4$) ions and (**b**) peak velocity, u_{PEAK}, corresponding to peak current shown in Figure 6 and of u_{HD} and u_q obtained as explained in Section 4.1.

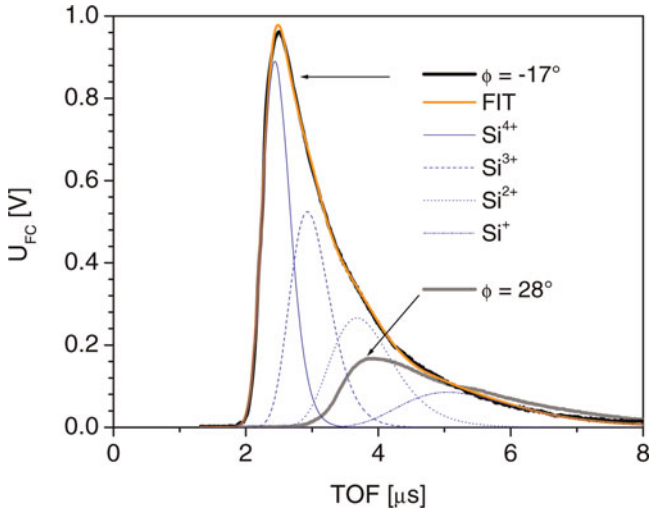

Fig. 9. (Color online) TOF spectra of Si ions observed at angles of 343° and 28° with respect to the target normal; $L_{FC} = 9$ cm. Uncovered partial ion currents are labelled as Si^{+} to Si^{4+} and their summa "FIT" is the fit by Eq. (5) to the observed TOF spectrum observed at $\phi = 343°$.

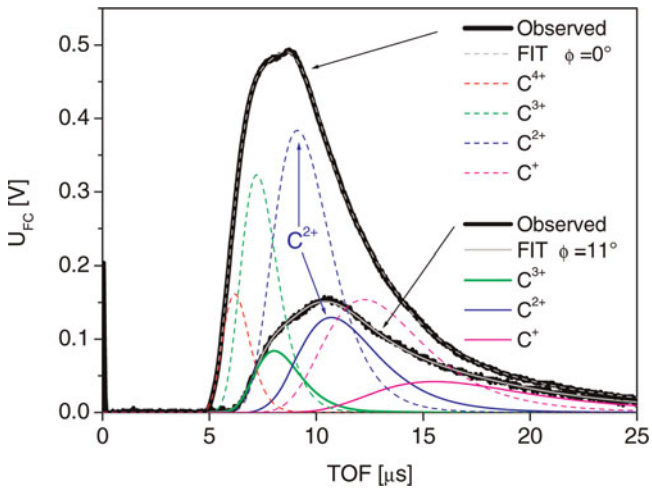

Fig. 10. (Color online) Time-of-flight spectra of C ions observed at angles of 0° and 11° with respect to the target normal; $L_{FC} = 24$ cm, $F = 12.5$ J/cm^2. The corresponding groups of uncovered partial ion currents are labelled as C^{+} to C^{4+} and C^{+} to C^{3+}.

5. CONCLUSION

The uncovering of partial currents of ionized species constituting the expanding plasma generated with the use of pulsed lasers allows the determination of the number of ions contained in the corresponding partial currents, the CM velocities, and the temperature. It was shown that the linear regression of the charge-state dependence of the CM velocity of thermal ions could be interpreted in terms of hydrodynamic and electrostatic forces ($u_{CM} = u_{HD} + u_q\ q$) balanced by collisions among ions, which result in the creation of a jet of plasma. The term u_{HD} of the CM velocity was ascribed to the effect of the hydrodynamic forces. The other term u_q related to the charge-state q is proportional to the ratio of the ambipolar field and the collisional frequency. The values of u_{HD} and u_q are comparable. In addition, the uncovering of partial ion currents observed in various directions also shows that the angular distribution of the expanding plasma is determined primary by the angular distribution of the ionization degree of the plasma plume. The CM velocity exhibits a slight angular distribution.

REFERENCES

Andreev, A., Platonov, K. & Kawata, S. (2009). Ion acceleration by short high intensity laser pulse in small target sets. *Laser Part. Beams* **27**, 449–457.

Badziak, J., Kozlov, A.A., Makowski, J., Parys, P., Ryc, L., Wolowski, J., Woryna, E. & Vankov, A.B. (1999). Investigations of ion streams emitted from plasma produced with a high-power picosecond laser. *Laser Part. Beams*, **17**, 323–329.

Bin, J.H., Lei, A.L., Yang, X.Q., Huang, L.G., Yu, M.Y., Yu, W. & Tanaka, K.A. (2009). Quasi-monoenergetic proton beam generation from a double-layer solid target using an intense circularly polarized laser. *Laser Part. Beams* **27**, 485–490.

Capitelli, M., Casavola, A., Colonna, G. & De Giacomo, A. (2004). Laser-induced plasma expansion: theoretical and experimental aspects. *Spectrochim. Acta Part B*, **59**, 271–289.

Doria, D., Lorusso, A., Belloni, F. & Nassisi, V. (2004). Characterization of a nonequilibrium XeCl laser-plasma by a movable Faraday cup. *Rev. Sci. Instrum.* **75**, 387–392.

Forslund, D. (1980). Coronal expansion with multiple charge states. In *Inertial fusion program: progress report*

https://doi.org/10.1017/S0263034611000103 Published online by Cambridge University Press

LA-7587-PR. Los Alamos: Los Alamos Scientific Laboratory, pp. 93–96.

Gitomer, S.J., Jones, R.D., Begay, F., Ehler, A.W., Kephart, J.F. & Kristal, R. (1986). Fast ions and hot electrons in the laser-plasma interactions. *Phys. Fluids* **29**, 2679–2688.

Haseroth, H. & Hora, H. (1996). Physical mechanisms leading to high currents of highly charged ions in laser-driven ion sources. *Laser Part. Beams*, **14**, 393–438.

Hora, H. (2007). New aspects for fusion energy using inertial confinement. *Laser Part. Beams* **25**, 37–45.

Kasperczuk, A., Pisarczyk, T., Kálal, M., Martínková, J., Ullschmied, J., Krouský, E., Mašek, K., Pfeifer, M., Rohlena, K., Skála, J. & Pisarczyk, P. (2008). PALS laser energy transfer into solid targets and its dependence on the lens focal point position with respect to the target surface. *Laser Part. Beams*, **28** 189–196.

Kasperczuk, A., Pisarczyk, T., Demchenko, N.N., Gus'kov, S.Yu., Kálal, M., Ullschmied, J., Krouský, E., Mašek, K., Pfeifer, M., Rohlena, K., Skála, J. & Pisarczyk, P. (2009). Experimental and theoretical investigations of mechanisms responsible for plasma jets formation at PALS. *Laser Part. Beams* **27**, 415–427.

Kelly, R. & Dreyfus, R.W. (1988). On the effect of Knudsen-layer formation on studies of vaporazation, sputtering, and desorption. *Surf. Sci.* **198**, 263–276.

Krása, J., Jungwirth, K., Krouský, E., Láska, L., Rohlena, K., Pfeifer, M., Ullschmied, J. & Velyhan, A. (2007). Temperature and centre-of-mass energy of ions emitted by laser-produced polyethylene plasma. *Plasma Phys. Control. Fusion* **49**, 1649–1659.

Krása, J., Velyhan, A., Jungwirth, K., Krouský, E., Láska, L., Rohlena, K., Pfeifer, M. & Ullschmied, J. (2009). Repetitive outbursts of fast carbon and fluorine ions from sub-nanosecond laser-produced plasma. *Laser Part. Beams* **27**, 241–248.

Láska, L., Badziak, J., Boody, F.P., Gammino, S., Jungwirth, K., Krása, J., Krouský, E., Parys, P., Pfeifer, M., Rohlena, K., Ryć, L., Skála, J., Torrisi, L., Ullschmied, J. & Wołowski, J. (2007*a*). Factors influencing parameters of laser ion sources. *Laser Part. Beams* **25**, 199–205.

Láska, L., Badziak, J., Gammino, S., Jungwirth, K., Kasperczuk, A., Krása, J., Krouský, E., Kubeš, P., Parys, P., Pfeifer, M., Pisarczyk, T., Rohlena, K., Rosiński, M., Ryć, L., Skála, J., Torrisi, L., Ullschmied, J., Velyhan, A. & Wołowski, J. (2007*b*). The influence of an intense laser beam interaction with preformed plasma on the characteristics of emitted ion streams. *Laser Part. Beams* **25**, 549–556.

Láska, L., Jungwirth, K., Krása, J., Krouský, E., Pfeifer, M., Rohlena, K., Velyhan, A., Ullschmied, J., Gammino, S., Torrisi, L., Badziak, J., Parys, P., Rosiński., M., Ryć, L. &Wołowski, J. (2008). Angular distributions of ions emitted from laser plasma produced at various irradiation angles and laser intensities. *Laser Part. Beams* **26**, 555–565.

Láska, L., Krása, J., Velyhan, A., Jungwirth, K., Krouský, E., Margarone, D., Pfeifer, M., Rohlena., K, Ryć., L, Skála., J, Torrisi., L. & Ullschmied, J. (2009). Experimental studies of generation of similar to 100 MeV Au-ions from the laser-produced plasma. *Laser Part. Beams* **27**, 137–147.

Liu, M.P., Xie, B.S., Huang, Y.S., Liu, J. & Yu, M.Y. (2009). Enhanced ion acceleration by collisionless electrostatic shock in thin foils irradiated by ultraintense laser pulse. *Laser Part. Beams* **27**, 327–333.

Lorusso, A., Krása, J., Rohlena, K., Nassisi, V., Belloni, F. & Doria, D. (2005). Charge losses in expanding plasma created by an XeCl laser. *Appl. Phys. Lett.* **86**, 081501.

Lorusso, A., Belloni, F., Doria, D., Nassisi, V., Krása, J. & Rohlena, K. (2006). Significant role of the recombination effects for a laser ion source. *J. Phys. D: Appl. Phys.* **39**, 294–300.

Miotello, A. & Kelly, R. (1999). On the origin of the different velocity peaks of particles sputtered from surfaces by laser pulses or charged-particle beams. *Appl. Surf. Sci.* **138–139**, 44–51.

Steinke, S., Henig, A., Schnürer, M., Sokollik, T., Nickles, P.V., Jung, D., Kiefer, D., Horlein, R., Schreiber, J., Tajima, T., Yan, X.Q., Hegelich, M., Meyer-Ter-Vehn, J., Sandner, W. & Habs, D. (2010). Efficient ion acceleration by collective laser-driven electron dynamics with ultra-thin foil targets. *Laser Part. Beams* **28**, 215–221.

Tajima, T. & Dawson, J. M. (1979). Laser electron accelerator. *Phys Rev. Lett.* **43**, 267–270.

Thum-Jäger, A. & Rohr, K. (1999). Angular emission distributions of neutrals and ions in laser ablated particle beams. *J. Phys. D: Appl. Phys.* **32**, 2827–2831.

Torrisi, L., Gammino, S. & Andò, L. (2002). Non-equilibrium plasma production by pulsed laser ablation of gold. *Radiat. Eff. Defects Solids*, **157**, 333–346.

Wilks, S.C., Langdon, A.B., Cowan, T.E., Roth, M., Singh, M., Hatchett, S., Key, M.H., Pennington, D., Mackinnon, A. & Snavely, R.A. (2001). Energetic proton generation in ultra-intense laser–solid interactions. *Phys. Plasmas* **8**, 542–549.